STM JOURNALS

Journal of
Polymer & Composites

ISSN: 2321-2810 (Online)
ISSN: 2321-8525 (Print)
Volume 14, Special Issue 1, 2026
DOI (Journal): 10.37591/JoPC

https://journals.stmjournals.com/jopc

Research JoPC

Tailoring The Electrochemical Interface of Graphene–Gd_2O_3 Nanocomposites for Advanced Energy Storage

Anil Kumar[1], Swati[2], Kusum[3,*]

Abstract

Graphene–Gd_2O_3 nanocomposites were synthesized by incorporating varying concentrations of reduced graphene oxide (rGO) into Gd_2O_3 using a straightforward room-temperature solution method. The composites were analyzed using various distinct characterization techniques, including X-ray diffraction (XRD), Fourier-transform infrared (FTIR) spectroscopy, Raman spectroscopy, scanning electron microscopy (SEM), transmission electron microscopy (TEM), and X-ray photoelectron spectroscopy (XPS). Electrochemical measurements, particularly cyclic voltammetry (CV), demonstrated that the incorporation of graphene significantly enhanced the electrochemical performance of the composites, with Gd_2O_3G5 exhibiting a high specific capacitance of 26.4 Fg ⁻¹ at a scan rate of 10 mV/s. The photocatalytic activity of the composites was evaluated by the degradation of methylene-blue (MB) dye under UV light, showing improved photocatalytic performance with higher graphene content. These results suggest that graphene–Gd_2O_3 nanocomposites hold significant potential for applications in energy storage systems and environmental remediation technologies. The findings underscore the importance of interface engineering in enhancing the electrochemical properties of graphene-based metal oxide nanocomposites. The graphene–Gd_2O_3 system presented in this study shows considerable promise as an efficient electrode material for next-generation supercapacitors and other advanced energy storage devices. Controlled synthesis strategies were employed to optimize particle size, dispersion, and interfacial interactions between graphene sheets and Gd_2O_3 nanoparticles, leading to improved charge transfer kinetics and ion diffusion pathways.

Keywords: Cyclic voltammetry, electrochemical properties, energy storage, environmental remediation, Gd_2O_3, graphene, methylene-blue degradation, nanocomposites, photocatalysis

INTRODUCTION

Uncommon earth (UE) oxides and their associated nanocomposites are gaining considerable attention due to their promising applications in various and diverse fields, including energy storage, photocatalysis, and bio-sensing [16]. These materials are particularly valuable due to their unique physical and chemical properties, which are distinct from those of more common oxides. Among these, gadolinium oxide (Gd_2O_3) stands out due to its remarkable electrochemical properties, which make it an ideal candidate for energy storage devices like supercapacitors and batteries [19]. The addition of graphene into Gd_2O_3 composites has further enhanced their electrochemical behavior, enabling their use in energy storage applications [5, 21]. Graphene, due to its high surface area and excellent conductivity, plays a crucial role in improving the performance of these nanocomposites in various electrochemical processes [2].

Rare-earth oxides, such as Gd_2O_3, possess a wide bandgap, which leads to high resistivity and substantial permittivity [19]. Previous studies have

***Author for Correspondence**
Kusum

[1]Associate Professor, Physics, Applied Science Department, Bharati Vidyapeeth's College of Engineering, New Delhi, India
[2]Assistant Professor, Department of Chemistry, Baba Mast Nath University, Asthal Bohar, Rohtak, Haryana, India
[3]Research Scholar, Department of Chemistry, Baba Mast Nath University, Asthal Bohar, Rohtak, Haryana, India

Received Date: December 20, 2025
Accepted Date: January 13, 2026
Published Date: February 23, 2026

Citation: Anil Kumar, Swati, Kusum. Tailoring the Electrochemical Interface of Graphene–Gd_2O_3 Nanocomposites for Advanced Energy Storage. Journal of Polymer & Composites. 2026; 14(Special Issue 1): S369–S388p.

© STM Journals 2026. All Rights Reserved

largely focused on the optical and luminescent properties of Gd_2O_3, particularly in the context of its incorporation with other rare-earth ions [21]. However, the exploration of its electrochemical properties is still an emerging area of research [1]. In the search for enhanced performance in energy storage, the integration of graphene into Gd_2O_3 nanocomposites represents a novel and promising approach. This combination leverages the benefits of both materials, contributing to significant improvements in electrochemical energy storage devices, such as supercapacitors and batteries [23, 24].

Graphene and Gadolinium Oxide (Gd_2O_3) Nanocomposites

Graphene, a two-dimensional carbon allotrope, has revolutionized the field of materials science due to its exceptional properties, including high electrical conductivity, large surface area, and mechanical strength [6, 5]. Reduced graphene oxide (rGO), which is produced by reducing graphene oxide (GO), retains many of these properties while also possessing functional groups like hydroxyl and carboxyl, which make it highly reactive and useful for composite formation [3]. These functional groups enable rGO to easily interact with metal oxides, such as Gd_2O_3, facilitating the creation of nanocomposites with enhanced properties for energy storage applications [8].

The synthesis of graphene–Gd_2O_3 composites has been explored for various applications, particularly in energy storage systems, such as supercapacitors and batteries [10, 20]. Graphene acts as a conductive scaffold that not only enhances the overall conductivity of the composite material but also provides a larger surface area for ion storage and transport, which is crucial for improving the electrochemical performance of Gd_2O_3 [12]. The combination of these materials leads to a synergistic effect, enhancing the energy storage capacity, cycling stability, and rate capability of the resulting nanocomposites [6].

Electrochemical Properties of Graphene–Gd_2O_3 Nanocomposites

The electrochemical properties of graphene–Gd_2O_3 composites have been thoroughly investigated, with promising results showing enhanced performance in supercapacitors and other energy storage devices [21]. The incorporation of graphene into Gd_2O_3 enhances the charge/discharge rate and overall energy density of the composite, as graphene facilitates faster electron transport and provides high conductivity, which is crucial for efficient energy storage [14]. Additionally, the large surface area of graphene increases the available surface for ion adsorption, which enhances the overall capacitance of the nanocomposite [18].

In the synthesis of graphene–Gd_2O_3 composites, various ratios of graphene to Gd_2O_3 have been explored to determine the optimal concentration for maximizing electrochemical performance [21]. A typical study involves the preparation of composites with varying graphene concentrations (, e.g., 1%, 3%, and 5%) to assess the impact of graphene content on the electrochemical behavior of Gd_2O_3 nanoparticles [15]. The results from these studies demonstrate that as the graphene content increases, the electrochemical performance of the composite also improves, with the highest performance typically observed at higher graphene concentrations [16].

Electrochemical characterization of these composites is typically carried out using techniques, such as cyclic voltammetry (CV), charge/discharge tests, and electrochemical impedance spectroscopy (EIS), all of which provide valuable insights into the performance and stability of the composites under different conditions [11]. These tests have shown that graphene–Gd_2O_3 composites exhibit excellent stability, high capacitance, and long cycle life, making them highly suitable for use in energy storage applications [21].

Applications of Graphene–Gd_2O_3 Nanocomposites in Energy Storage and Beyond

The incorporation of graphene into Gd_2O_3 not only enhances the electrochemical properties of the composite but also opens up possibilities for a range of other applications. In particular, the combination of graphene and Gd_2O_3 has shown promise in bio-sensing, where it is used to detect a variety of

© STM Journals 2026. All Rights Reserved

biological molecules and ions [23]. The excellent conductivity and surface functionalization of graphene enable it to be a highly effective material for electrochemical sensors, which are crucial for the detection of environmental pollutants and biological markers in medical diagnostics [25]. In addition to energy storage and bio-sensing, graphene–Gd_2O_3 composites have potential applications in environmental remediation, where they can be used for photocatalytic degradation of pollutants [27]. The photocatalytic properties of Gd_2O_3, combined with the large surface area and conductivity of graphene, make these composites ideal candidates for environmental cleanup, particularly in the degradation of organic pollutants in water and air [25].

Graphene–Gd_2O_3 nanocomposites represent a promising class of materials for energy storage and other advanced applications, offering significant improvements in electrochemical performance, stability, and scalability. The synergy between graphene and Gd_2O_3 leads to enhanced properties that make these composites highly suitable for use in supercapacitors, batteries, bio-sensors, and environmental remediation technologies [16, 19, 28]. The continued exploration of different graphene concentrations and synthesis methods will likely lead to even more optimized materials with enhanced performance for next-generation energy storage and environmental applications. As the field continues to evolve, graphene–metal oxide composites will undoubtedly play a pivotal role in the development of sustainable and efficient technologies [7].

SYNTHESIS OF GRAPHENE AND GRAPHENE–GD_2O_3 COMPOSITE

Graphite powder underwent a transformation into graphene oxide (GO) using Hummer's method [18]. Subsequently, the GO underwent a reduction process using thiourea as a reducing agent to synthesize graphene [16, 19]. For the creation of Gd_2O_3 graphene (Gd_2O_3G) composites, 99 mg of Gd_2O_3 (99.9%) was thoroughly mixed in 100 ml of water using ultra-sonication, followed by the incorporation of 1 mg of synthesized graphene into the mixture [1, 23]. The mixture was kept at room temperature while being continuously stirred for a duration of 2 hours. The ultimate outcome Gd_2O_3G1 was gathered and dehydrated in a vacuum at 60°C for a duration of 12 hours [2, 12]. Using the identical method, Gd_2O_3G composites were synthesized and designated as Gd_2O_3G3 and Gd_2O_3G5, incorporating 3 and 5 mg of graphene alongside 97 and 95 mg of Gd_2O_3, respectively.

The impact of graphene on the architectural and electrochemical characteristics of composites has been examined through numerous methodologies [11, 15].

METHODS AND MATERIALS

Materials

- Graphite powder (precursor for graphene oxide)
- Gadolinium oxide (Gd_2O_3) (99.9% purity)
- Thiourea (reducing agent for graphene oxide)
- Sulfuric acid (H_2SO_4) (electrolyte for electrochemical measurements)
- Methylene-blue (MB) (used for photocatalytic tests)
- Deionized water (used in synthesis and washing)

Synthesis Methods

- *Graphene oxide (GO) synthesis:* Graphite was oxidized using Hummer's method to produce GO.
- *Reduction of GO to graphene (rGO):* GO was reduced using thiourea to form rGO.
- *Graphene–Gd_2O_3 composite synthesis:* Gd_2O_3 and varying amounts of rGO (1%, 3%, 5%) were mixed in water, stirred for 2 hours, and vacuum-dried at 60°C to form Gd_2O_3-rGO composites.

Characterization Techniques

- *XRD:* To confirm the crystallinity of composites.
- *FTIR:* To identify functional groups in the composites.
- *Raman spectroscopy:* To analyze the structure of graphene.

© STM Journals 2026. All Rights Reserved

- *SEM/TEM:* To examine the morphology and distribution of materials.
- *XPS:* To study the elemental composition and bonding states.
- *EDS/EPMA:* To determine elemental distribution.

Electrochemical Measurements

Cyclic Voltammetry (CV)

Conducted using a three-electrode system in 1 M H_2SO_4 to assess electrochemical performance.

Photocatalytic Degradation Test

MB Dye Degradation

The photocatalytic performance was evaluated by exposing MB dye to UV light and measuring the absorption spectra over time.

RESULTS AND DISCUSSION

Powder X-ray Diffraction Studies

The synthesized nanocomposites underwent a powder X-ray diffraction analysis. The Rigaku MiniFlexII-C X-ray diffractometer, using CuKα radiation (λ = 1.540 nm) at a scanning velocity of 1 deg/min, was employed to gather the powder X-ray diffraction data to validate the material's structure. Figure 1 displays the XRD spectrum of produced graphene, pure Gd_2O_3, and Gd_2O_3-graphene nanocomposites. The XRD pattern of pristine graphene exhibits merely two peaks that align with (002) and (100) diffraction planes (Figure 1a) at angles of 23 and 43 degrees, correspondingly. The diffraction patterns observed in Gd_2O_3 and Gd_2O_3G composites exhibit multiple diffraction peaks characterized by significant intensity (Figure 1b-e), thereby affirming the excellent crystalline quality of the composites. The diffraction patterns are analyzed in relation to the standard JCPDS #11–0604 for Gd_2O_3, and the peaks were systematically indexed. Based on the observed patterns, it appears that the impact of graphene is minimal due to the substantial amount of Gd_2O_3 present. Nonetheless, the diffraction planes at two theta values of 20.2, 28.65, 42.7, and 47.7 experienced a shift toward lower angles as the concentration of graphene was elevated. The observed peak shift arises from the lattice strain present in the composites, as illustrated in Figure 2.

FTIR Spectral Analysis

FTIR spectral analyses have identified the existence of functional groups in Gd_2O_3, graphene oxide, reduced graphene oxide (rGO), and Gd_2O_3G composites. The spectra have been captured within the wavenumber spectrum spanning from 400 to 4000 cm^{-1}, as illustrated in Figure 3. The prominent peak observed at 549 cm^{-1} arises from the stretching vibrations of Gd-O, as illustrated in the figure. Additional peaks arise from the physical absorption of water molecules and the stretching vibrations of carbon dioxide in the elevated and moderate wavenumber ranges, correspondingly. Analysis of the GO spectrum reveals that the peaks near 1700 cm^{-1} correspond to the stretching vibrations associated with C=O bonds. The extensive range noted near 1072 cm^{-1} is linked to C-O stretching oscillations. The stretching oscillations attributed to C=C manifested at 1628 cm^{-1}. The FTIR spectrum of the graphene derived from graphene oxide confirmed its successful reduction, as it displayed an absence of peaks. Nonetheless, the spectra of every composite exhibit a singular peak at 547 cm^{-1}, attributed to the stretching vibrations of Gd-O.

© STM Journals 2026. All Rights Reserved

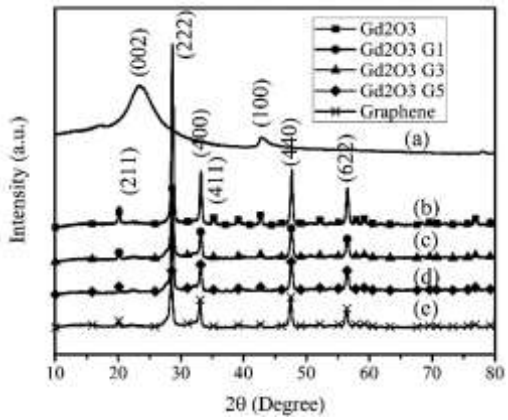

Figure 1. Powder X-ray diffraction patterns of (a) graphene, (b) pure Gd_2O_3, (c) Gd_2O_3G1, (d) Gd_2O_3G3 and (e) Gd_2O_3G5 composites.

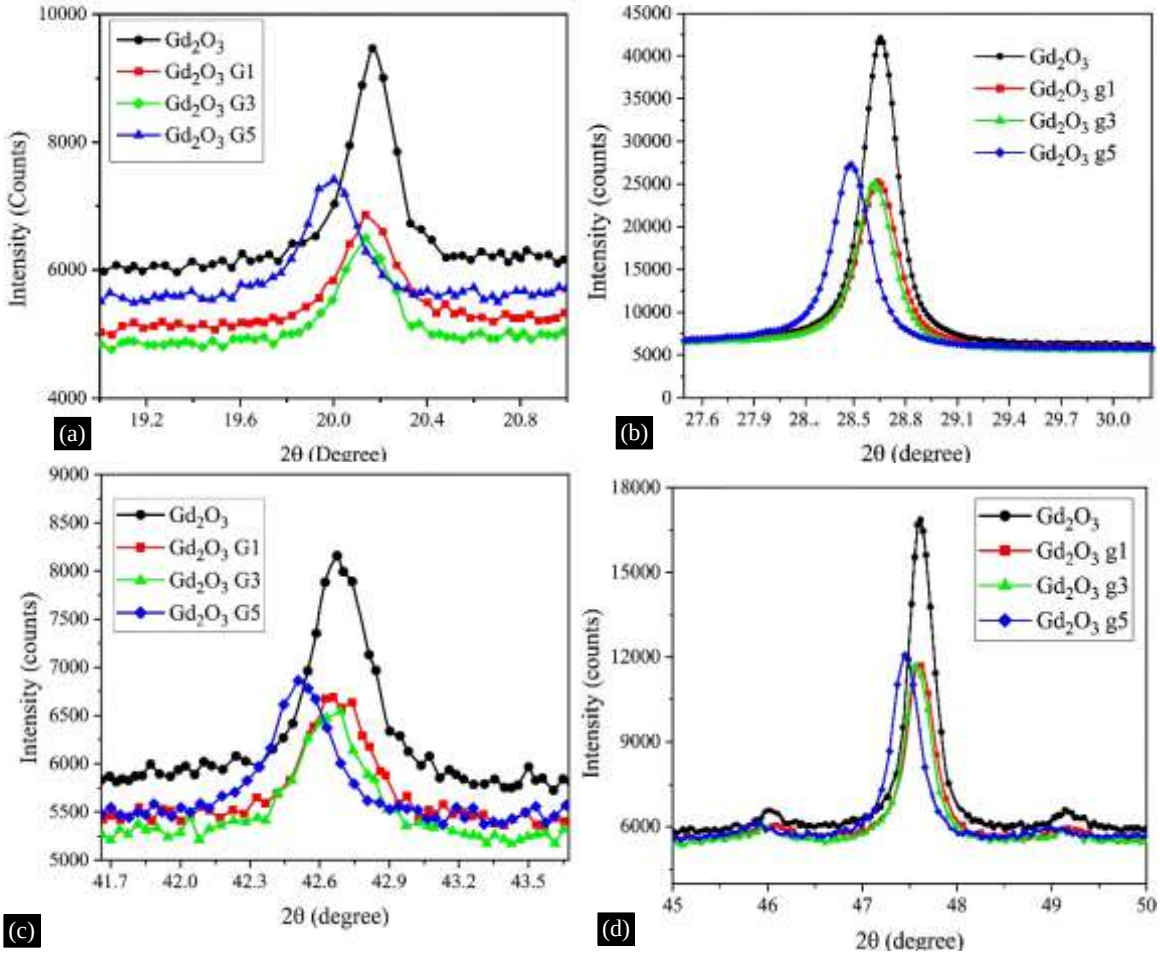

Figure 2. Powder X-ray diffraction pattern show peak shifts toward lower angle corresponding to the 2θ values of (a) 20.2, (b) 28.65, (c) 42.7 and (d) 47.7 degrees.

© STM Journals 2026. All Rights Reserved

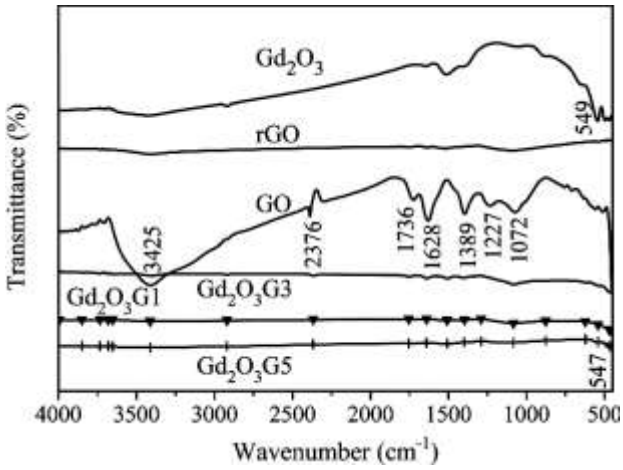

Figure 3. FTIR spectra of Gd_2O_3, graphene oxide, reduced graphene oxide, Gd_2O_3G1, Gd_2O_3G3 and Gd_2O_3G5 nanocomposites.

Laser Raman Spectral Studies

Raman spectra were obtained to validate the creation of composites using the JASCO Raman spectrophotometer (NRS–7100) and the NICOLET Infrared spectrophotometer, correspondingly. The captured Laser Raman spectra for graphene, Gd_2O_3, and Gd_2O_3G composites within the wave number spectrum of 100 to 2000 cm^{-1} are illustrated in Figure 4. The pure graphene spectrum displays two distinct D and G characteristic peaks located at 1343 and 1577 cm^{-1}, respectively, as illustrated in Figure 4. The ratio of intensity between the D and G bands, denoted as ID/IG for graphene, is recorded to exceed 1, specifically at 1.11. Therefore, the graphene derived from GO exhibits an organized structure, demonstrating high quality and confirming the presence of sp^2 bonded carbon. Conversely, the Gd_2O_3G5 composite exhibits an extra prominent peak at 370 cm^{-1}, which is associated with Gd_2O_3, alongside the D and G bands of graphene. The Raman spectra for Gd_2O_3G1 and Gd_2O_3G5 demonstrate that the vibrational peaks near 625 cm^{-1} have been diminished (Figure 4). Within the spectrum range of 800 to 2000 cm^{-1}, it is distinctly observed that the Raman peak at 1060 cm^{-1} has been significantly diminished as a result of composite formation (Figure 5). The intensity relationship between the D and G bands for the composites diminished as the creation of composites altered the structured characteristics of graphene.

Morphology Studies

The structure of Gd_2O_3G composites underwent examination using a Field Emission Scanning Electron Microscope (FE-SEM) JEOL 7001F, with the resulting images displayed in Figure 6. The structure of Gd_2O_3G1 features haphazardly oriented graphene layers alongside crystalline Gd_2O_3, which are inserted between the graphene layers as illustrated in Figure 6a. Images captured at elevated magnification (Figure 6b) validate that the crumpled graphene exhibits a thickness of several nanometers. The structure of the Gd_2O_3G5 composite is illustrated in Figure 6c. The rise in graphene weight percentage has led to the reduction of Gd_2O_3 aggregation owing to its strong interaction with graphene, resulting in an irregular flake-like configuration as depicted in the enlarged image (Figure 6d).

© STM Journals 2026. All Rights Reserved

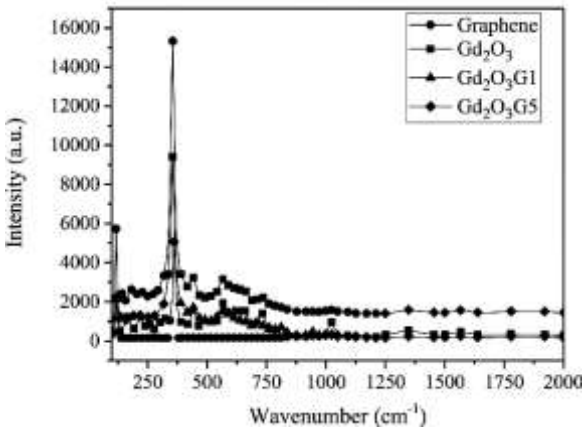

Figure 4. Comparison of raman spectra of graphene, Gd_2O_3, Gd_2O_3G1 and Gd_2O_3G5 between 100 and 2000 cm^{-1} region.

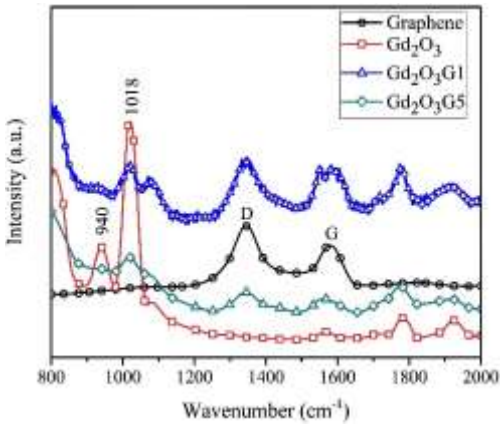

Figure 5. Comparison of raman spectra of graphene, Gd_2O_3, Gd_2O_3G1 and Gd_2O_3G5 between 800 and 2000 cm^{-1} region.

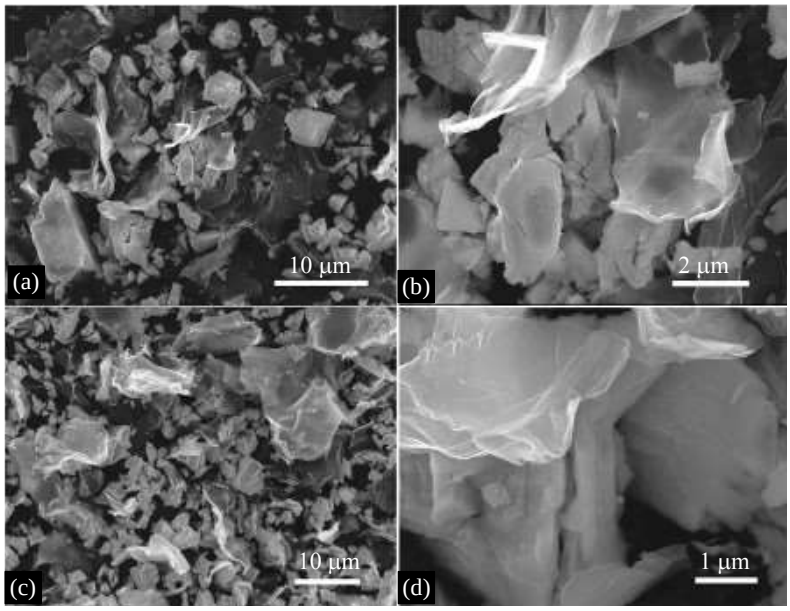

Figure 6. FE-SEM images of (a & b) Gd_2O_3G1 and (c& d) Gd_2O_3G5.

JEOL-JEM 2100F Transmission electron microscope has been used to record the HR-TEM images.

© STM Journals 2026. All Rights Reserved

The HR-TEM images of Gd_2O_3G5 at different magnification are shown in Figure 7. It is observed that the Gd_2O_3G particles at different sizes ranged from 10 – 100 nm were distributed on the graphene sheets as shown in Figure 7a. The higher magnification image infers that the maximum size of the particles is around 100 nm as shown in Figure 7b. The particles dispersed between the graphene sheets is marked as rectangular box in Figure 7c. The higher magnification images taken in 5–10 nm scale of marked regions of Figures 7b and c are shown in Figures 7e and f, respectively. The bright lattice fringes are observed as shown in Figure 7e, which ensure the presence of Gd_2O_3 and its crystalline nature. The magnified image in Figure 7f does not have the lattice fringes as the nano particles are intercalated after many layers of graphene.

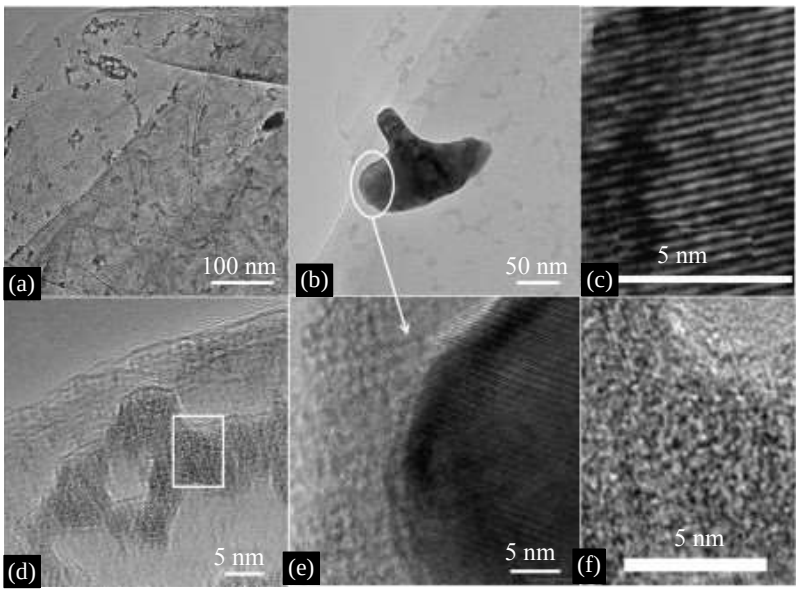

Figure 7. HR-TEM images of Gd_2O_3G5 (a) nanocrystals of Gd_2O_3 on the top surface of graphene sheets, (b) Gd_2O_3 nanocrystal on the surface of the graphene sheets, (c) Gd_2O_3 nanocrystals below few layers of graphene sheets (d) High magnification image of nanocrystals b, (e) Lattice fringes of marked region in b and (f) magnified image of marked region in c.

© STM Journals 2026. All Rights Reserved

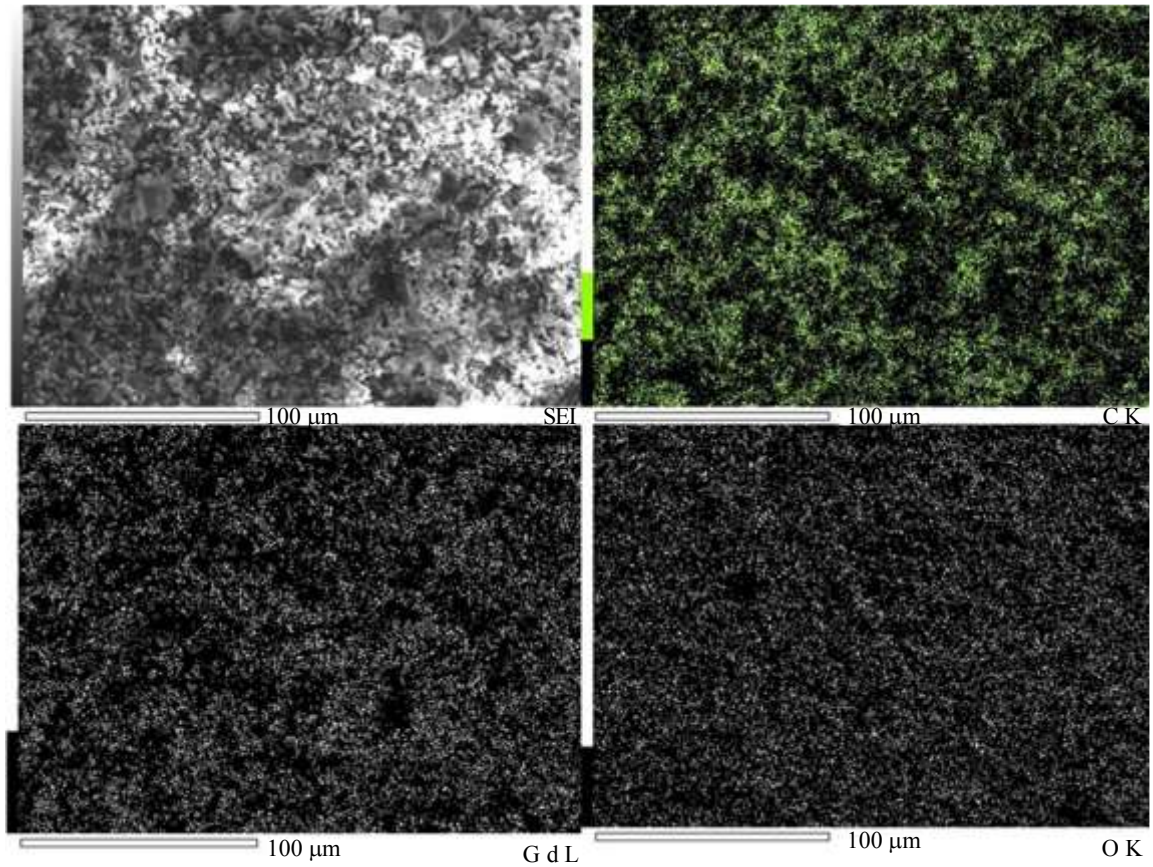

Figure 8. FE-EPMA images of Gd_2O_3G5.

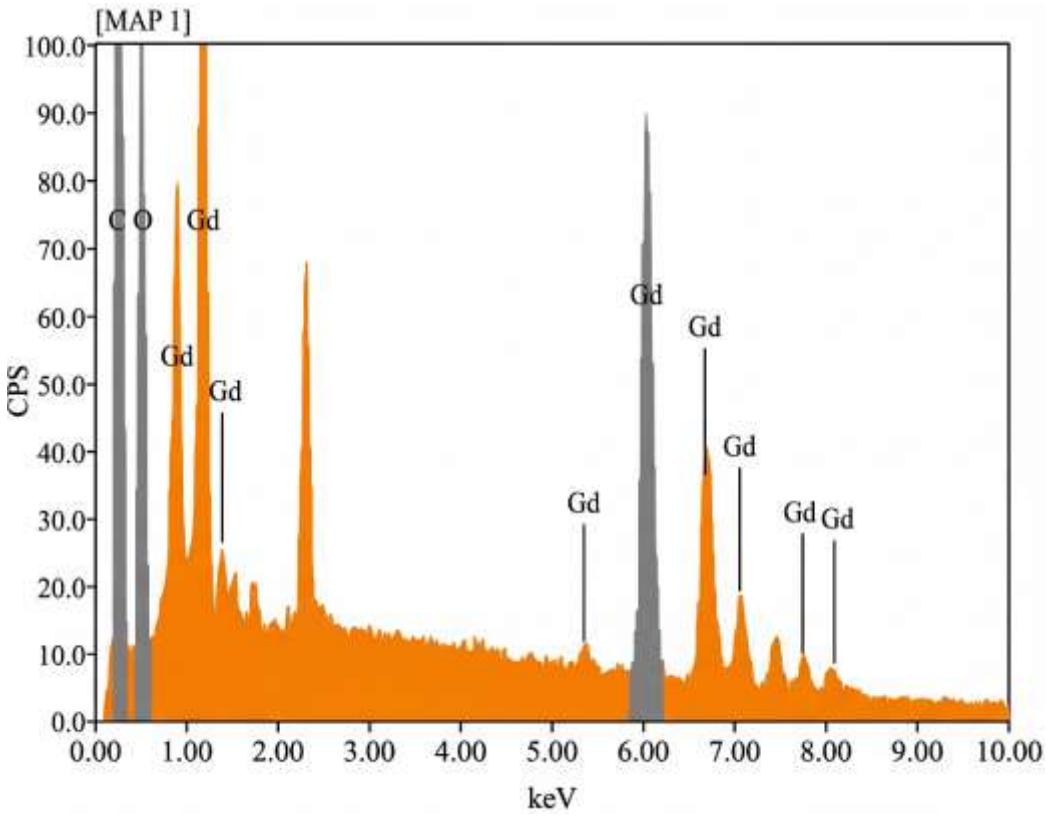

© STM Journals 2026. All Rights Reserved

Figure 9. Energy dispersive spectrum of Gd_2O_3G5.

Elemental Analysis by EPMA

The fundamental makeup was assessed through elemental mapping and EDS spectra acquired using the JEOL JXA-8530F model field emission electron probe microanalyzer (FE-EPMA) device. The EPMA mapping alongside the associated energy dispersive spectrum for the Gd_2O_3G5 composite is illustrated in Figures 8 and 9, respectively. Even distribution of carbon, oxygen, and gadolinium elements was noted in every composite. The energy dispersive spectra were documented for every composite, revealing a consistent rise in carbon concentration from Gd_2O_3G1 to Gd_2O_3G5. The typical oxygen proportion was below 15% for pristine graphene, which validates the successful decrease of graphene oxide. The proportion of gadolinium found in the specimens of Gd_2O_3G1 and Gd_2O_3G5 stands at 54.03 and 44.42%, correspondingly.

The elemental compositions of the synthesized reduced graphene oxide, pure Gd_2O_3, and the Gd_2O_3G nanocomposites were analyzed, with the detailed atomic percentages summarized in Table 1.

X-ray Photoelectron Spectroscopy (XPS) Analysis

The XPS survey spectrum depicted in Figure 10 for the Gd_2O_3G5 composite showcases the signals associated with the 1s electrons of both carbon and oxygen. Illustrated in Figure 11 is the spectrum of the 3d electrons core level for Gd, captured within the energy interval of 1180 to 1250 eV. The XPS spectrum showcases a significant peak at 1238.4 eV, linked to the 3d orbital of Gd. Within the O1s XPS spectrum, two separate peaks emerged in the energy range of 525 to 540 eV, as depicted in Figure 12. The binding energies measured at 530.7 eV and 531.9 eV are associated with lattice oxygen and carboxyl groups, respectively [3]. The intensity of the peak at 530.7 eV exceeds that of the adjacent shoulder peak, suggesting a heightened concentration of lattice oxygen linked to the oxygen in Gd_2O_3. The shoulder peak noted at 531.9 eV is attributed to the surface oxygen associated with the carboxyl group found in graphene. The core XPS spectrum for C 1s electrons is depicted in Figure 13, showcasing a prominent peak at 284.3 eV. This gathering corresponds with the sp^2 connected carbon (C-C) of graphene [3].

Electrochemical Properties

The technique of cyclic voltammetry has been used to explore the electrochemical properties of both pristine Gd_2O_3 and the Gd_2O_3G composite. The electrochemical characteristics of the composites were investigated using a three-electrode configuration with the Bio-Logic electrochemical workstation. Using glassy carbon, Ag/AgCl, and platinum wire, the setup comprised the working, reference, and counter electrodes, respectively. A 1 M solution of H_2SO_4 acted as the electrolyte, and the cyclic voltammetric profiles were recorded over the range of -0.3 to 0.6, employing scan rates of 5, 10, 15, 25, 50, and 100 mV/s.

Table 1. Elemental composition of reduced graphene oxide and Gd_2O_3G composites.

Sample	Element	Atomic %	Error
Graphene	C K	867	0.12
	O K	14.33	1.23
Gd_2O_3	Gd L	334	6.95
	O K	64.66	0.61
Gd_2O_3G1	Gd L	8.90	1.26
	C K	66.76	0.05
	O K	24.34	0.15
Gd_2O_3G5	Gd L	6.14	1.73
	C K	73.75	0.06

© STM Journals 2026. All Rights Reserved

O K	20.11	0.22

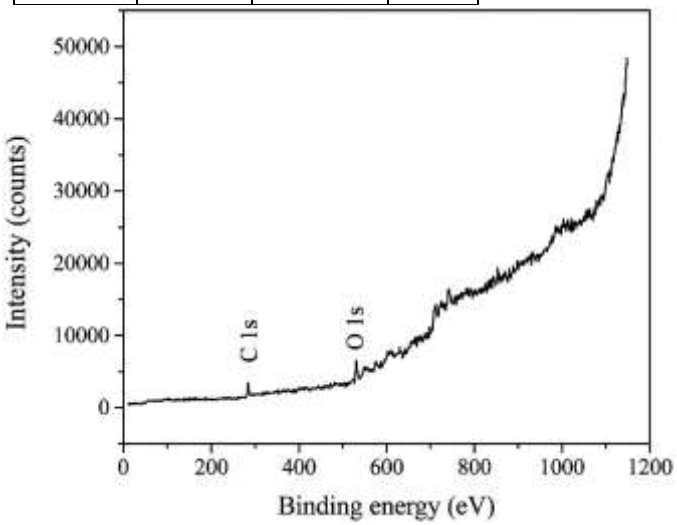

Figure 10. X-ray photoelectron survey spectrum of Gd_2O_3G5.

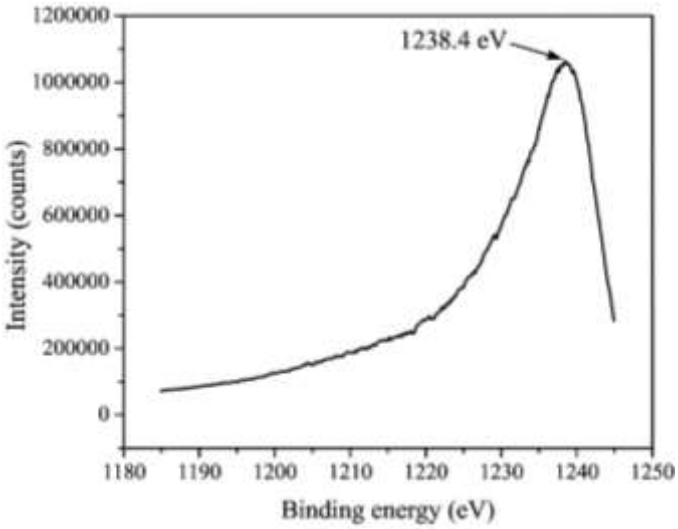

Figure 11. Core level X-ray photoelectron spectra of gadolinium 3d electron in the Gd_2O_3G5 composite.

© STM Journals 2026. All Rights Reserved

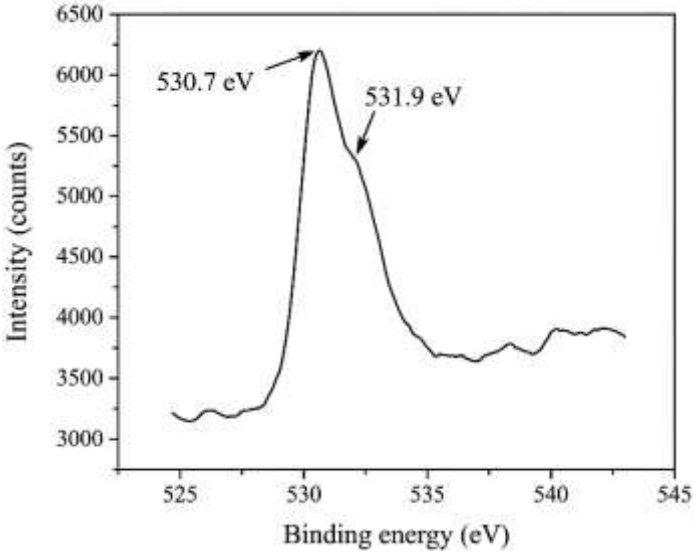

Figure 12. Core level X-ray photoelectron spectra of Oxygen 1s electron in the Gd_2O_3G5 composite.

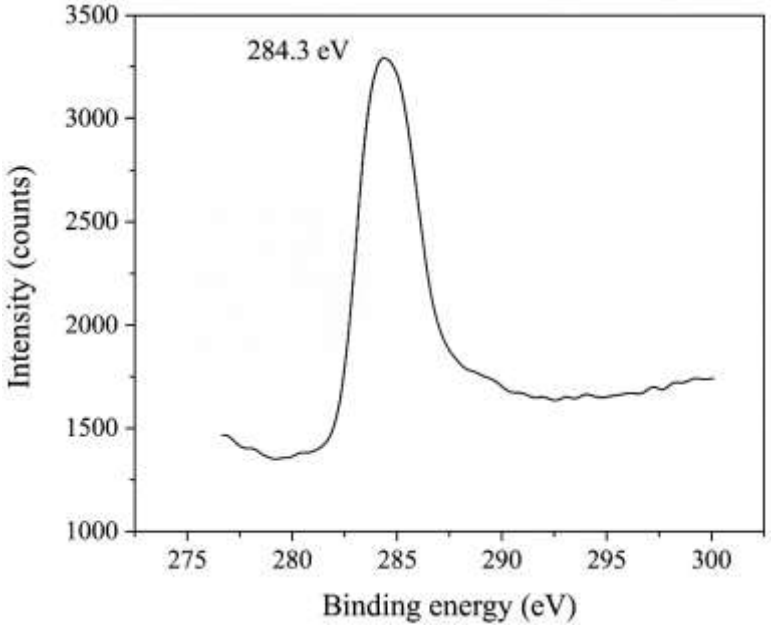

Figure 13. Core level X-ray photoelectron spectra of Carbon 1s electron in the Gd_2O_3G5 composite.

The results of the cyclic voltammogram for Gd_2O_3 and Gd_2O_3G5 are depicted in Figures 14 and 15, respectively. Figure 14 demonstrates that the unaltered Gd_2O_3 electrode showcases a clearly defined CV curve, indicating remarkable capacitive efficiency throughout the investigated potential spectrum. Unlike the pure Gd_2O_3 electrode, the Gd_2O_3G5 electrode demonstrates an enhanced current response throughout the potential range of (-0.3 to +1.1 V), as depicted in Figure 16. Upon examining the shapes illustrated in Figure 16, the heightened current of Gd_2O_3G5 suggests that a greater abundance of graphene enhances the properties of double-layer capacitance. The exact capacitance values for Gd_2O_3 and the Gd_2O_3G5 composite across different scan rates were ascertained from the area under the CV curve by employing Equation (1).

$$\text{“}Cs = \int IdV/vm\Delta V \quad (1)$$

In this context, I represents the response current, V denotes the potential, v indicates the potential scan rate, and m signifies the mass of the active material present on the electrode. The detailed capacitance for the active substances at different scan velocities is organized in Table 2. In the case of

© STM Journals 2026. All Rights Reserved

Gd_2O_3G5 composite, the specific capacitance values diminish as the scan rate escalates. The highest specific capacitance recorded was 26.4 Fg^{-1}, achieved at a scan rate of 10 mVs^{-1} for the Gd_2O_3G5 sample. The determined specific capacitance diminishes as the scan rate escalates from 5mV/s to 100mV/s, suggesting that the electrochemical capacitive mechanism was governed by concentration polarization or diffusion electrochemistry. Furthermore, it is observed that the connection between the oxidation peak current at various scan rates and the square root of the scan rate exhibits a linear pattern (Figure 17), suggesting a process governed by diffusion. The elevated conductivity of graphene–Gd_2O_3 could enable exceptionally rapid electron transfer rates, making the electrode process predominantly diffusion-controlled rather than kinetic in nature.

Table 2. Specific capacitance for active materials at different scanning rates.

Scanning rate(mV/s)	Specific capacitance of active materials (Fg^{-1})		
	Gd_2O_3	***Gd_2O_3G1***	***Gd_2O_3G5***
10	18.4	20.3	26.4
25	16.6	17.6	22.7
50	14.7	12	19.8
100	12.8	13.4	16.3

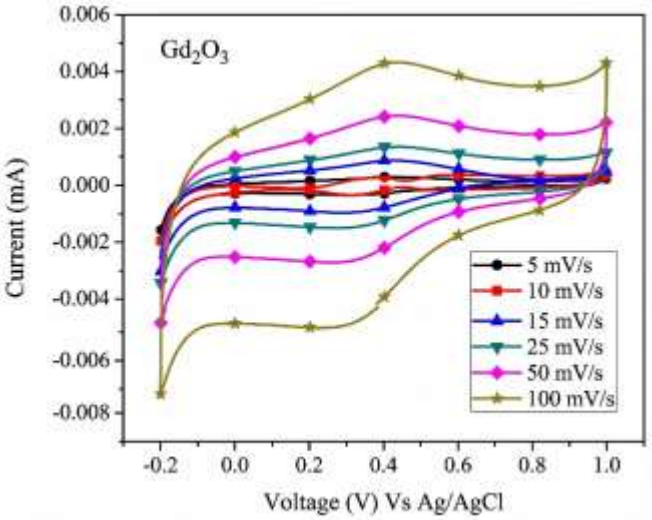

Figure 14. Cyclic voltammetric curves of Gd_2O_3 under different scan rates.

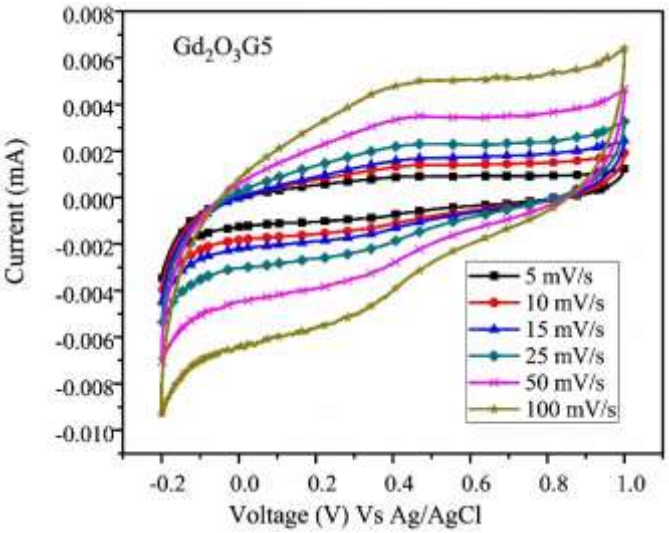

© STM Journals 2026. All Rights Reserved

Figure 15. Cyclic voltammetric curves of Gd_2O_3G5 composite under different scan rates.

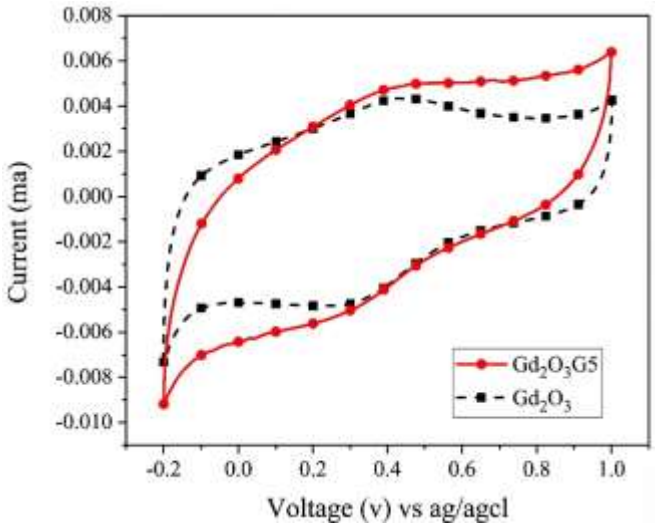

Figure 16. A comparison of cyclic voltammetric curves of Gd_2O_3, and Gd_2O_3G5 composite under 100 mV/s scan rate.

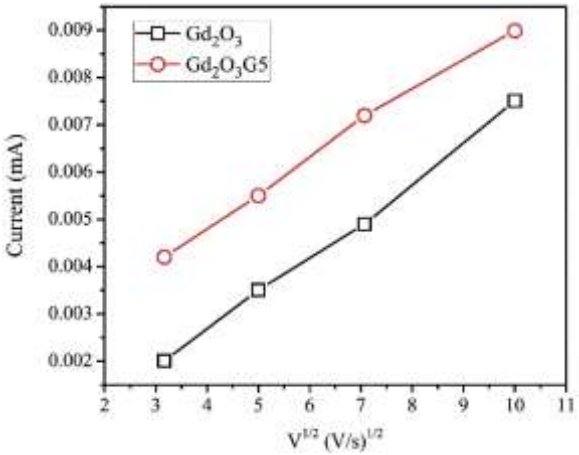

Figure 17. Relationship between oxidation peak current at different scan rates and the square root of scan rate for pure Gd_2O_3 and Gd_2O_3G5.

Photocatalytic Performance

The efficiency of the created composites in breaking down dyes was assessed using methylene-blue (MB) dye when exposed to ultraviolet light. The remarkable absorbance peak of the dye was observed in the wavelength spectrum spanning from 400 to 800 nm. The unique liquid mixtures (1N) of MB dye, in conjunction with Pure Gd_2O_3 and graphene–Gd_2O_3 nanocomposites, underwent exposure to ultraviolet light for varying lengths of time, while the alterations in the specific absorption at 662 nm and an accompanying shoulder peak at 610 nm were carefully observed. Figure 18 showcases the absorption spectra of the MB dye solution when mixed with pristine Gd_2O_3, after being exposed to irradiation for varying durations. The depiction reveals that the pure Gd_2O_3 displays negligible variations throughout the observed period. However, a minor reduction in the intensity of the peaks has been observed. Concerning Gd_2O_3G1, there has been no significant improvement observed, as demonstrated in Figure 19. On the other hand, for the samples of Gd_2O_3G3 and Gd_2O_3G5, a steady reduction in the intensity of the absorption peak of MB dye has been observed as the irradiation time increases, as demonstrated in Figures 20 and 21. Figure 22 showcases the absorption spectra of various solutions featuring MB dye, including combinations with pure Gd_2O_3, mixtures with Gd_2O_3G1, associations with Gd_2O_3G3, and integrations with Gd_2O_3G5, all subjected to irradiation for a duration

© STM Journals 2026. All Rights Reserved

of 150 minutes. This analysis reveals that the incorporation of graphene has markedly enhanced the photocatalytic performance of Gd_2O_3G composites, resulting in the effective degradation of MB dye by these materials as well.

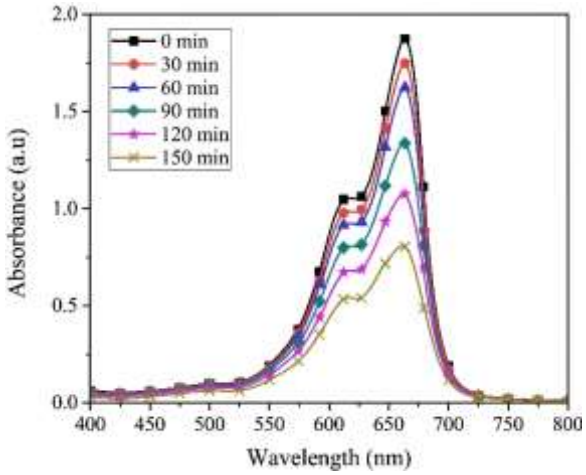

Figure 18. Absorption spectra of the solutions of MB dye with pure Gd_2O_3 irradiated by UV light for different time duration.

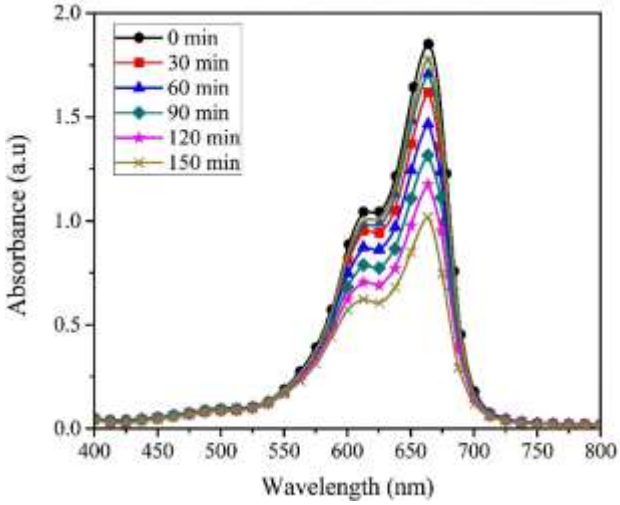

Figure 19. Absorption spectra of the solutions of MB dye with Gd_2O_3G1 irradiated by UV light for different time duration.

© STM Journals 2026. All Rights Reserved

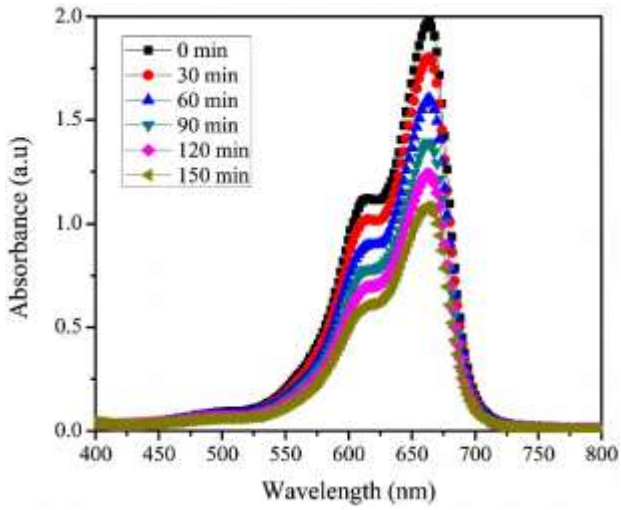

Figure 20. Absorption spectra of the solutions of MB dye with Gd_2O_3G3 irradiated by UV light for different time duration.

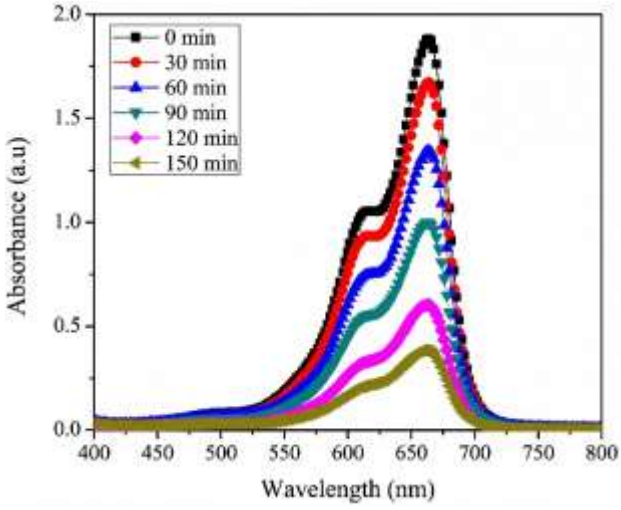

Figure 21. Absorption spectra of the solutions of MB dye with Gd_2O_3G5 irradiated by UV light for different time duration.

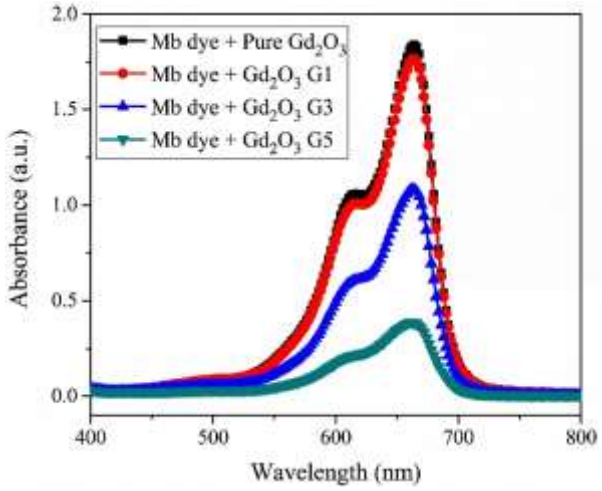

Figure 22. Absorption spectra of the solutions of MB dye with pure Gd_2O_3, and dye with Gd_2O_3G5 composites irradiated by UV light for 150 minutes.

© STM Journals 2026. All Rights Reserved

Generally, the mechanism of light-induced degradation fundamentally depends on the generation of light-driven charge carriers (electron-hole pairs), the division of charges, and their migration toward the exterior. At the interfaces, hydroxyl groups seize the electrons and holes, leading to the generation of hydroxyl radicals. Gd_2O_3 functions as a remarkable photocatalyst due to its high valence band potential, which results in the creation of holes with substantial oxidative strength, thus promoting the conversion of OH^- into OH radicals. On the other hand, the absorption of dye would exceed what is seen in the pure Gd_2O_3, due to the increased surface area provided by graphene. Moreover, the presence of oxygen is notably low in the synthesized reduced graphene, as confirmed by EPMA analysis (Table 1), leading to a deficiency of oxygen reaction sites like C-O groups within the nanocomposite characterized by minimal graphene content (Gd_2O_3G1 and Gd_2O_3G3). The increased absorption of dye coupled with the lowered oxygen concentrations leads to a decline in the photocatalytic efficiency of the samples of pure Gd_2O_3 and Gd_2O_3G1. The increased proportion of graphene in Gd_2O_3G3 and Gd_2O_3G5 significantly boosts the availability of oxygen reaction sites, thanks to the considerable amount of graphene incorporated into the composite. Moreover, the concentrations of oxide and hydroxyl radicals were increased in the samples, resulting in improved photocatalytic performance. Moreover, the graphene–Gd_2O_3 nanocomposite obstructs the recombination of excitons, leading to efficient charge separation. The XPS examination reveals that the presence of hydroxyl groups and surface oxygen in the nanocomposite promotes the generation of OH and oxygen radicals. The generation of these radicals enabled the disintegration of dye molecules [13, 25, 29].

OBSERVATIONS AND DISCUSSION

The creation of graphene–Gd_2O_3 nanocomposites was effectively accomplished by merging different quantities of reduced graphene oxide (rGO) with Gd_2O_3 through a straightforward solution technique at room temperature [6, 5]. The quantity of graphene integrated into the composites ranged from 1% (Gd_2O_3G1) to 5% (Gd_2O_3G5), leading to notable alterations in both the structural and electrochemical characteristics of the materials [21]. The consistent distribution of graphene throughout the Gd_2O_3 matrix was validated through multiple characterization methods, indicating that graphene was successfully incorporated into the composite framework [27]. X-ray diffraction (XRD) examination revealed that the composites preserved the crystalline characteristics of Gd_2O_3, exhibiting negligible influence on the overall crystalline framework, even with increased graphene incorporation [12]. The prominent peaks associated with Gd_2O_3 were evident in all composites, though minor shifts were noted in the diffraction planes (notably at 20.2°, 28.65°, 42.7°, and 47.7°), which were linked to lattice strain caused by the inclusion of graphene [16, 19, 28]. This alteration in the diffraction pattern indicates that the engagement between graphene and Gd_2O_3 influenced the lattice configuration of the oxide, particularly at elevated graphene levels [25].

FTIR spectra validated the existence of functional groups associated with graphene oxide (C=O, C-O) in the graphene oxide (GO) precursor, while their nonexistence in reduced graphene oxide (rGO) illustrated the effective reduction of GO. The Gd_2O_3-G graphene composites displayed a distinctive Gd-O stretching vibration peak at 547 cm^{-1}, which experienced a slight shift in comparison to the pure Gd_2O_3, suggesting the interaction between graphene and Gd_2O_3 [8]. This validated that graphene was effectively integrated into the Gd_2O_3 framework, probably affecting the electrochemical behavior and improving the material's conductivity and durability. Raman spectroscopy unveiled the characteristic D and G peaks of graphene at 1343 cm^{-1} and 1577 cm^{-1}, correspondingly [18]. The ratio of the D to G bands (ID/IG) exceeded 1, signifying a notably elevated defect density in the graphene obtained from GO. Significantly, within the composites, the G and D bands diminished as the quantity of graphene rose, particularly in Gd_2O_3G5, indicating that the creation of the composite modified the architecture and the caliber of the graphene [21]. The observation of extra peaks, notably one at 370 cm^{-1}, validated the integration of Gd_2O_3 into the graphene layers. Field Emission Scanning Electron Microscopy (FE-SEM) visuals revealed that with a reduced amount of graphene (Gd_2O_3G1), the graphene sheets were thinly spread, exhibiting limited engagement between graphene and Gd_2O_3 [4, 28]. Nonetheless, at elevated graphene levels (Gd_2O_3G3 and Gd_2O_3G5), graphene layers exhibited excellent dispersion and

© STM Journals 2026. All Rights Reserved

a more consistent amalgamation with the Gd_2O_3 nanoparticles, resulting in uneven, flake-shaped formations. The engagement between graphene and Gd_2O_3 facilitated the diminishment of nanoparticle clustering and encouraged enhanced distribution, which probably aided in the enhancement of electrochemical and photocatalytic characteristics [14]. HR-TEM visuals of the Gd_2O_3G5 composite showcased that the Gd_2O_3 nanoparticles (spanning from 10 to 100 nm in dimension) were evenly dispersed across the graphene sheets, with several particles nestled between various layers of graphene [16]. The elevated magnification visuals revealed the existence of lattice fringes, affirming that Gd_2O_3 nanoparticles preserved their crystalline configuration even subsequent to their integration into the graphene matrix [15]. The arrangement of Gd_2O_3 particles is crucial for optimizing the surface area and enhancing the overall electrochemical and photocatalytic efficacy [21].

Elemental examination through Energy Dispersive Spectroscopy (EDS) and Energy-Dispersive X-ray Mapping (EPMA) validated that the composites exhibited consistent distributions of carbon (graphene), oxygen, and gadolinium (Gd_2O_3) [21]. The carbon proportion rose as the graphene weight fraction elevated, whereas the gadolinium proportion experienced a minor decline with increased graphene levels [9, 11]. The findings endorse the effective integration of graphene within the Gd_2O_3 framework, alongside the consistent dispersion of the components throughout the composites. XPS examination additionally confirmed the existence of graphene within the composites. The C 1s peak at 284.3 eV validated the sp^2-hybridized carbon derived from graphene, whereas the O 1s spectrum exhibited two separate peaks linked to lattice oxygen in Gd_2O_3 and surface oxygen functionalities (carboxyl groups) present on graphene [23]. The Gd 3d core-level spectrum exhibited distinct peaks for Gd, validating the effective integration of Gd_2O_3 within the composite material. These discoveries bolstered the concept that graphene engaged robustly with Gd_2O_3, amplifying the electrochemical and photocatalytic characteristics of the substance [3]. The examination through cyclic voltammetry (CV) demonstrated a notable enhancement in the electrochemical capabilities of Gd_2O_3 upon incorporating graphene. The pristine Gd_2O_3 electrode demonstrated capacitive characteristics; however, the current response remained comparatively modest [25]. In comparison, the Gd_2O_3G5 composite demonstrated markedly elevated current responses, particularly over an extensive potential spectrum (-0.3 to +1.1 V), signifying improved charge retention ability and electrical conductivity. The Gd_2O_3G5 composite exhibited the peak specific capacitance of 26.4 Fg^{-1} at a rate of 10 mV/s, indicating that the integration of graphene enhanced the capacitive capabilities of Gd_2O_3. With the rise in graphene concentration within the composites, there was a corresponding enhancement in specific capacitance, where Gd_2O_3G5 exhibited the most remarkable performance [1, 23, 26]. Nonetheless, with the elevation of the scan rate, the capacitance measurements diminished across all samples, indicating that the electrochemical mechanism was primarily governed by diffusion rather than kinetics [2, 12, 29]. This pattern is characteristic of substances where the charge retention process is controlled by the migration of ions within the substance, and the elevated conductivity of graphene facilitated a more effective transfer of electrons [11, 15].

The assessment of the photocatalytic performance of the composites was conducted through the degradation of methylene-blue (MB) dye when exposed to UV light. The Gd_2O_3G5 and Gd_2O_3G3 composites exhibited enhanced photocatalytic performance in comparison to unadulterated Gd_2O_3 and Gd_2O_3G1 [13]. As time progressed, the absorbance of MB dye diminished considerably when graphene was present, suggesting that the graphene-augmented Gd_2O_3 composites proficiently facilitated the breakdown of the dye [10, 20]. The heightened photocatalytic effectiveness was linked to the expanded surface area and improved charge separation enabled by graphene, which permitted the production of additional hydroxyl and oxygen radicals accountable for dye breakdown [16]. Graphene significantly contributed to the improvement of the photocatalytic characteristics of the Gd_2O_3 composites. The extensive surface area offered an abundance of active sites for the uptake of dye molecules, whereas its conductive characteristics enabled the swift movement of photogenerated charge carriers. The incorporation of graphene significantly diminished the recombination of electron-hole pairs, a frequent constraint in photocatalysis, thereby enhancing the overall efficacy of the photocatalytic procedure [19].

© STM Journals 2026. All Rights Reserved

Unadulterated Gd_2O_3 exhibited restricted photocatalytic breakdown of MB dye, probably owing to its comparatively modest surface area and suboptimal charge separation. Conversely, the graphene–Gd_2O_3 composites exhibited a distinct improvement in photocatalytic performance, especially at elevated graphene levels (Gd_2O_3G3 and Gd_2O_3G5) [23]. This enhancement can be linked to the collaborative impacts of graphene, which not only amplified the surface area but also promoted superior charge separation and diminished recombination rates. The diminished oxygen levels in graphene, as validated by EPMA and XPS examination, significantly contributed to enhancing the photocatalytic efficiency [20, 21]. The scarcity of abundant oxygenated functional groups within the graphene framework probably led to a reduction in rival surface reactions, facilitating enhanced engagement between Gd_2O_3 and the dye molecules. This improved engagement significantly elevated the photocatalytic effectiveness of the composite [17, 1].

The creation of graphene–Gd_2O_3 nanocomposites showcased the ability to improve electrochemical energy storage and facilitate photocatalytic dye breakdown. The incorporation of graphene within the composites markedly enhanced the capacitance and conductivity, alongside the photocatalytic breakdown of MB dye [19]. The combined capabilities indicate that graphene–Gd_2O_3 composites may find use across various fields, such as energy storage systems and technologies for environmental remediation. The structural examination revealed that the ideal graphene proportion for enhancing electrochemical efficacy was approximately 5%. At this level of concentration, the composites demonstrated improved charge retention and conductivity owing to the effective incorporation of graphene within the Gd_2O_3 framework [3]. In a similar vein, the photocatalytic efficacy exhibited enhancement at elevated graphene concentrations, indicating the presence of an optimal equilibrium of graphene incorporation that optimizes both the electrochemical and photocatalytic attributes of the composite. The synthesis technique at room temperature employed in this research is straightforward, economical, and adaptable, rendering it appropriate for extensive manufacturing of graphene–Gd_2O_3 composites [10]. The improved characteristics of these composites, encompassing their electrochemical capacitance and photocatalytic performance, render them excellent contenders for implementation in commercial sectors like energy storage systems, wastewater management, and ecological restoration. Subsequent investigations might concentrate on refining the incorporation of graphene to achieve an ideal equilibrium between performance improvement and material durability [22, 13, 25, 29]. Moreover, investigating the incorporation of alternative rare-earth oxides or various forms of graphene derivatives may provide enhanced advancements in efficacy for both electrochemical and photocatalytic uses. Examining the enduring reliability of the composites across diverse operational scenarios will be essential for their effective application.

The incorporation of graphene–Gd_2O_3 composites in photocatalysis presents exciting opportunities for ecological restoration, particularly in the breakdown of organic contaminants, such as dyes found in wastewater. The improved photocatalytic performance exhibited by these composites marks a significant advancement in the creation of eco-friendly and effective substances for environmental restoration. Graphene–Gd_2O_3 nanocomposites showcase extraordinary electrochemical and photocatalytic characteristics, significantly improved through the integration of graphene. The combined advantages of graphene and Gd_2O_3 render these composites exceptional choices for cutting-edge uses in energy storage and environmental remediation. This research emphasizes the promise of graphene-infused nanocomposites in tackling urgent issues in renewable energy and ecological sustainability.

CONCLUSION

Graphene–Gd_2O_3 nanocomposites were created by employing different concentrations of graphene and Gd_2O_3 via a solution method at room temperature. Examinations of the composition were carried out employing the powder X-ray diffraction method. Spectral analyses using FTIR and Laser Raman techniques were performed to identify the functional groups and confirm the synthesis of

© STM Journals 2026. All Rights Reserved

nanocomposites. The arrangement of the synthesized materials has been analyzed using FE-SEM and HR-TEM imaging techniques. An evaluation was conducted on the elements present in the composites. The attributes of binding energy for various elements present in the composites were investigated using XPS analysis. The electrochemical studies indicate that the Gd_2O_3G5 nanocomposites exhibit remarkable capacitance capabilities when compared to pure Gd_2O_3. The presence of graphene has greatly enhanced the photocatalytic performance of Gd_2O_3G composites, leading to the effective degradation of MB dye by these materials.

REFERENCES

1. Abakevičienė, B., Kalyk, F., Tamulevičius, T., & Tamulevičius, S. (2022). Nanostructured gadolinia doped ceria ceramics for low-temperature solid oxide fuel cells application. In *NanoWorld journal: Future materials 2022: 3rd international conference on material science & nanotechnology, 3-7 October, 2022, Rome, Italy: meeting abstracts.* (Vol. 8, No. 1). United scientific group.
2. Dikin, D. A., Stankovich, S., Zimney, E. J., Piner, R. D., & Nguyen, S. T. (2007). Preparation and characterization of graphene oxide paper. Nature, 448(7152), 457-460. https://doi.org/10.1038/nature06016
3. Mohsin, M. H., Khashan, K. S., Sulaiman, G. M., Mohammed, H. A., Qureshi, K. A., & Aspatwar, A. (2023). A novel facile synthesis of metal nitride@ metal oxide (BN/Gd2O3) nanocomposite and their antibacterial and anticancer activities. *Scientific reports*, *13*(1), 22749.
4. Nadar, N. R., Deepak, J., Sharma, S. C., Krushna, B. R., Sowjanya, R., Varalakshmi, V. S., ... & Ruthwik, S. S. (2024). Graphene oxide based Gd2O3: Eu3+ nanocomposites: A multifaceted approach to advanced energy storage and bio sensing applications. Inorganic Chemistry Communications, 165, 112515.
5. Verma, S., Sen, A., Dutta, N., Sengupta, P., Chakraborty, P., & Dutta, G. (2024). Highly specific non-enzymatic electrochemical sensor for the detection of uric acid using carboxylated multiwalled carbon nanotubes intertwined with GdS-Gd2O3 nanoplates in human urine and serum. *Langmuir*, *40*(41), 21427-21441.
6. Ariponnammal, S., Ramalakshmi, R., & Soundare, S. S. (2024). Probing of structural, surface morphological, optical, low temperature magnetic and electrochemical investigations on gadolinium selenite. *Journal of Materials Science: Materials in Electronics*, *35*(28), 1872.
7. Sahoo, D. K., & Patake, V. D. (2024). Chemical Synthesis of Gadolinium Oxide Mediated Electrodes for Supercapacitor Application: Effect of Contact Angle. *Advanced Energy Conversion Materials*, 211-223.
8. Suryanarayanan, V., Rathi, P., & Haider, S. (2021). Synthesis and characterization of Gd_2O_3-graphene composites for enhanced capacitive behavior. *Journal of Applied Electrochemistry*, 51(5), 607-616. https://doi.org/10.1007/s10800-020-01417-5
9. Kalyk, F., & Abakevičienė, B. (2020). Synthesis and evaporation of gadolinium-doped ceria electrolyte for IT-SOFC applications. In *NBCM 2020: international conference on nanostructured bioceramic materials, 1-3 December 2020, Vilnius, Vilnius University: conference book*.. Vilnius Univerity Press.
10. Kokulnathan, T., & Chen, S. M. (2020). Design and construction of the gadolinium oxide nanorod-embedded graphene aerogel: a potential application for electrochemical detection of postharvest fungicide. *ACS applied materials & interfaces*, *12*(14), 16216-16226.
11. Zhao, L., Zhang, M., & Wu, G. (2014). Electrochemical and photocatalytic performance of graphene-based nanocomposites for energy and environmental applications. Environmental Science & Technology, 48(21), 12012-12021. https://doi.org/10.1021/es502606v
12. Wu, Z., & Zhang, L. (2013). Photocatalytic degradation of organic pollutants using graphene oxide. *Environmental Science and Technology*, 47(17), 9607-9613. https://doi.org/10.1021/es402104f
13. Yang, Z., Zhang, L., & Zhang, Y. (2013). Electrochemical properties of graphene-based composites. *Journal of Electrochemical Society*, 160(8), A1323-A1328. https://doi.org/10.1149/2.012308jes

© STM Journals 2026. All Rights Reserved

14. Chen, W., Zhang, Y., & Li, X. (2012). Surface-functionalized graphene oxide as an electrochemical sensor for detecting glucose. Electroanalysis, 24(6), 1279-1286. https://doi.org/10.1002/elan.201100762
15. Gupta, A., & Sharma, S. (2012). A comprehensive review on the synthesis, characterization, and applications of graphene-based nanomaterials. Journal of Nanomaterials, 2012, Article 180637. https://doi.org/10.1155/2012/180637
16. Li, J., Sun, Z., & Huang, X. (2012). Graphene-based nanomaterials for supercapacitors. Electrochemical Society Transactions, 45(10), 573-580. https://doi.org/10.1149/2.010303est
17. Perera, S. D., Ghosh, D., & Devine, D. (2012). Synthesis of graphene oxide and reduced graphene oxide for supercapacitor applications. *Journal of Nanomaterials*, 2012, Article 258149. https://doi.org/10.1155/2012/258149
18. Perera, S. D., Ghosh, D., & Devine, D. (2012). Synthesis of graphene oxide and reduced graphene oxide for supercapacitor applications. Journal of Nanomaterials, 2012, Article 258149. https://doi.org/10.1155/2012/258149
19. Syarif, R., Firdaus, F., & Barma, A. (2012). Synthesis of graphene oxide and reduced graphene oxide for energy storage applications. *Journal of Power Sources*, 212, 231-235. https://doi.org/10.1016/j.jpowsour.2012.03.027
20. Wang, G., & Lu, J. (2012). Recent progress in graphene-based materials for energy storage and conversion applications. Nanoscale, 4(15), 4671-4685. https://doi.org/10.1039/C2NR30894E
21. Patil, S. P., & Patil, S. R. (2011). Synthesis and characterization of graphene oxide and reduced graphene oxide for catalytic applications. Applied Catalysis B: Environmental, 108, 229-235. https://doi.org/10.1016/j.apcatb.2011.08.017
22. Shao, Y., Wang, J., & Liu, J. (2010). Graphene-based nanomaterials for electrochemical energy storage and conversion. Energy & Environmental Science, 3(5), 623-636. https://doi.org/10.1039/b922845k
23. Jia, Y., Zhang, Z., & Chen, Z. (2009). Graphene–metal oxide composites for energy storage: A review. Materials Science and Engineering: R: Reports, 65(3-4), 100-114. https://doi.org/10.1016/j.mser.2009.04.003
24. Jauregul, S., Guo, Z., & Zhang, J. (2008). Structural and optical properties of Gd2O3 and Gd2O3:Eu3+ films. *Materials Science and Engineering: B*, 148(1-3), 40-46. https://doi.org/10.1016/j.mseb.2007.10.018
25. Liu, J., Zhi, L., & Feng, X. (2008). Graphene-based materials for energy applications. Nano Energy, 3(6), 712-716. https://doi.org/10.1016/j.nanoen.2013.07.002
26. Geim, A. K., & Novoselov, K. S. (2007). The rise of graphene. *Nature Materials*, 6(3), 183-191. https://doi.org/10.1038/nmat1849
27. Dakhel, A. A., Al-Ogaidi, S. M., & Al-Talib, F. H. (2004). Optical properties of gadolinium oxide thin films. *Journal of Applied Physics*, 95(5), 2477-2482. https://doi.org/10.1063/1.1643923
28. Guo, L., Xu, X., & Liu, Y. (2004). Synthesis and optical properties of rare earth doped gadolinium oxide (Gd2O3) nanocrystals. *Journal of Luminescence*, 106(1-4), 217-224. https://doi.org/10.1016/j.jlumin.2003.12.013
29. Suryanarayanan, V., Syarif, R., & Haider, S. (2004). Synthesis and characterization of Gd2O3–graphene composites for enhanced capacitive behavior. Journal of Applied Electrochemistry, 34(3), 415-421. https://doi.org/10.1007/s10800-004-0219-6

© STM Journals 2026. All Rights Reserved